On the use of mass-conserving wind fields in chemistry-transport models

B. Bregman, A. Segers, M. Krol, E. Meijer, P. van Velthoven

**Atmospheric
Chemistry
and Physics
Discussions**

On the use of mass-conserving wind fields in chemistry-transport models

B. Bregman[1], A. Segers[1], M. Krol[2], E. Meijer[1], and P. van Velthoven[1]

[1]Royal Netherlands Meteorological Institute, P.O. Box 201, 3730 AE, De Bilt, Netherlands
[2]Institute for Marine and Atmospheric Research Utrecht, Princetonplein 5, 3584 CC, Netherlands

Correspondence to: B. Bregman (bregman@knmi.nl)

Abstract

A new method has been developed that provides mass-conserving wind fields for global chemistry-transport models. In previous global Eulerian modeling studies a mass-imbalance was found between the model mass transport and the surface pressure tendencies. Several methods have been suggested to correct for this imbalance, but so far no satisfactory solution has been found. Our new method solves these problems by using the wind fields in a spherical harmonical form (divergence and vorticity) by mimicing the physics of the weather forecast model as closely as possible. A 3-D chemistry-transport model was used to show that the calculated ozone fields with the new processing method agree remarkably better with ozone observations in the upper troposphere and lower stratosphere. In addition, the calculated age of air in the lower stratosphere show better agreement with observations, although the air remains still too young in the extra tropical stratosphere.

1. Introduction

Mass conservation is a fundamental requirement in global model integrations, both in chemistry-transport models (CTMs), which use external meteorological fields (the 'off-line' mode), and in general circulation models (GCMs), in which the transport is calculated ('on-line' mode). Changes in surface pressure should be consistent with the air mass changes within the model. However, in most models the vertically integrated mass change is not in balance with the surface pressure during a model time step, so that the fluxes need to be corrected.

There are several causes for this imbalance.

- The mass fluxes and surface pressure fields are independently calculated so that mass changes in the model do not necessarily balance the surface pressure tendency. This applies to both CTMs and GCMs.

– Interpolation of the original spectral data to the desired model grid with different time and spatial resolutions. This especially applies to models that use external wind fields to drive the transport.

– Inaccuracies in the horizontal mass fluxes due to the use of hybrid σ-pressure vertical coordinates. Surface pressure changes may lead to vertical mass fluxes if the vertical model layers have varying pressures.

– The use of meteorological fields that consist of analysis, which represent a mix between model results and observations, leading to mass flux imbalance. The way to solve this is to utilize 6-hourly forecasts instead of analysis.

– The differences between model integration time intervals and the discrete time steps at which meteorological fields are available. This inevitably leads to mass imbalance, and generally applies to models that use external meteorological fields. The reader is referred to Jöckel et al. (2001) for a detailed overview of potential causes of mass inconsistence in global chemistry-transport and climate models.

Various correction methods have been employed to achieve mass balance. Stockwell and Chipperfield (1999) applied a local tracer mass correction at hybrid σ-pressure layers. Jöckel et al. (2001) discussed the 'mass-fixer' problem in flux-form advection schemes and reported a two-step model grid adjustment to correct for the mass imbalance. They demonstrated that corrections may lead to (spurious) variations in tracer concentrations, particularly in the case of pronounced vertical gradients.

The most consistent correction for the mass imbalance is achieved when they are performed on the horizontal mass fluxes. This was done by Heimann and Keeling (1989) and Heimann (1995) who provided mass-conserving mass fluxes in their 3-D tracer model version 2 (TM2). The correction method they applied is referred to in this work as the 'old' method and described in more detail in Sect. 2.

Bregman et al. (2001) also used this correction method in the next version of the tracer model (TM3). However, they found significantly higher modeled ozone fields in

the lower(most) stratosphere than observed, which they attributed partly to errors in the mass fluxes by interpolation of the spectral meteorological fields to the Cartesian model grid (the second cause mentioned in the first paragraph). To solve this, they included the vertical mass fluxes directly from the meteorological fields and corrected
5   the horizontal mass fluxes accordingly. This gave much better agreement with observations in the winter, but worse in summer. Moreover, this correction method could not be applied at pressure levels higher than 300 hPa. Therefore another solution had to be found.

In this work we report a new method for mass flux processing to solve the mass-
10   imbalance problem. This method is designed for CTMs, minimizes interpolation errors and accounts for surface pressure changes in a consistent manner.

We have performed two types of model experiments to evaluate the processing method. One involves the calculation of the mean age of air, and the second consists of integrations with an ozone tracer version of the model. We will show that, by
15   using the new method, both the observed age of air and ozone fields are significantly better represented by the model.

In the following section we describe the tracer model and the old and new mass flux processing methods. Section 3 contains a description of the model experiment and presents the results of the model evaluation. The vertical air mass fluxes have been
20   analyzed in Sect. 4 to explain the model results. This is followed by conclusions.

2.   Model description

The global Tracer Model Version 3 (TM3) used in this study is a grid point 3-D Chemistry-Transport Model (CTM), originally developed by Heimann (1995); Heimann and Keeling (1989). Different versions of TM3 have been developed and validated recently (Den-
25   tener et al., 1999; Peters et al., 2001; Houweling et al., 1998; Van den Broek et al., 2000) 6-Hourly forecasts of the European Centre for Medium-range Weather Forecasts (ECMWF) are used to drive the transport. The model contains a Cartesian grid with a

Mass conservation in global models

B. Bregman et al.

horizontal resolution of 2.5° × 2.5°. It further contains 31 hybrid σ-pressure levels with the top level at 10 hPa. The vertical resolution varies with altitude, being hundred to a few hundred meters in the troposphere, one kilometer around the tropopause gradually increasing to a few kilometers close to the model top. The tracers are advected using
5 second-order moments (Prather, 1986). More detailed model description can be found elsewhere (Bregman et al., 2001).

The processing of the mass fluxes is performed using the 'old' and 'new' method, described in the following subsections.

2.1. Old method

10 In the old processing method the horizontal mass fluxes were derived from ECMWF spectral data, gridded on a 1° × 1° resolution. The horizontal mass fluxes [kg s^{-1}], $\mathbf{\Phi}_h = (\Phi_u, \Phi_v)$ are balanced with the surface pressure tendency by adding 'small' correction fluxes $\mathbf{F} = (F_u, F_v)$, to the vertically integrated horizontal mass fluxes shown in Eq. (1):

$$\delta_h \cdot \mathbf{F} = -\left[m_s(t_1) - m_s(t_0)\right]/\Delta t - \sum_{l=1}^{nlev} [\delta_h \cdot \mathbf{\Phi}_h(l)] \tag{1}$$

15

with m_s the air mass [kg] of the grid column, defined by the surface pressure p_s, the grid cell area (A), and the acceleration gravity of g ($m_s = p_s A/g$). δ_h is a discrete equivalent of the horizontal difference operator, which is the horizontal gradient operator, ∇, multiplied by the horizontal distance between the grid boundaries.

20 The correction field, $\mathbf{F}$, needed for mass balance is calculated by changing Eq. (1) into a Poisson equation, which is solved by discrete Fourier Transform (Heimann and Keeling, 1989; Heimann, 1995) (see also Segers et al., 2002a,b, for details). $\mathbf{F}$ is distributed over the vertical grid layers, l, weighted arbitrarily with the magnitude of the uncorrected horizontal mass fluxes. By this method errors in the horizontal mass fluxes

arise due to (i) interpolation and (ii) the arbitrarily vertical distribution of F, which lacks a realistic physical interpretation.

2.2. New method

In the new processing method the above mentioned problems have been solved. For mass balance the divergence, vorticity, and surface pressure are needed. For the surface pressure we have used the natural logarithm ($\ln p_s$), since this is used by the ECMWF model. The new processing method requires that these quantities are retrieved in the original model representation, i.e. in spherical harmonics. The method is described in detail by Segers et al. (2002a) and Segers et al. (2002b).

The horizontal mass fluxes [kg s^{-1}], $\mathbf{\Phi}_h = (\Phi_u, \Phi_v)$ are obtained by integrating the spectral fields over the grid boundaries in the following equations.

$$\Phi_u = \frac{R}{g} \int_{\Delta\beta_i} \frac{U(\lambda, \beta, k)}{\cos\beta} \, \Delta p_k \, \mathrm{d}\beta \tag{2}$$

$$\Phi_v = \frac{R}{g} \int_{\Delta\lambda_i} V(\lambda, \beta, k) \, \Delta p_k \, \mathrm{d}\lambda \tag{3}$$

In here, λ is the longitude, β the latitude, $\Delta p_k = \Delta a_k + \Delta b_k p_s$ the pressure gradient over a model level k with a_k and b_k the hybrid coefficients, and $(U, V) = (u, v)\cos\beta$, a scaled velocity vector. The latter is easy to compute in spectral form from spectral vorticity and divergence. R represents the radius of the earth [m] and g the acceleration of gravity.

As described above, these mass fluxes should be consistent with the surface pressure p_s [Pa], which is calculated from its spectral representation by surface integration

in Eq. (4).

$$p_s = \iint\limits_{A} p_s(\lambda, \beta) \, \cos\beta \, \mathrm{d}\lambda \, \mathrm{d}\beta \, / \, A \tag{4}$$

The vertical mass fluxes $\mathbf{\Phi}_w$ [kg s^{-1}] for a level k are calculated by vertical integration of the mass divergence and pressure gradients:

$$\Phi_w = \frac{R^2}{g} \iint\limits_{A_i} \left[\left(\sum_{j=1}^{n_{lev}} \Omega_j \right) b_{k+1/2} \; - \; \sum_{j=1}^{k} \Omega_j \right] \cos\beta \, \mathrm{d}\beta \, \mathrm{d}\lambda \tag{5}$$

where

$$\Omega_j \; = \; D_j \, (\Delta a_j + \Delta b_j p_s) \; + \; \frac{\mathbf{V}_j}{\cos\beta} \cdot \left(\mathbf{\nabla}(\ln p_s) \right) p_s \, \Delta b_j \tag{6}$$

Here $\Omega = \mathbf{\nabla} \cdot (\mathbf{v} \cdot \Delta p)$ and represents the horizontal mass divergence [kg s^{-1}]. It is computed from the 'velocity divergence' $D_j = \nabla \cdot \mathbf{v}$ [s^{-1}], and the horizontal gradient of the surface pressure ($\nabla \ln p_s$). The latter arises because of orography and is relevant for models with vertical hybrid σ-pressure levels. For models with plain pressure levels the second term on the right in Eq. (6) can be omitted, since $\Delta b_j = 0$. $\nabla \ln p_s$ can also be derived from $\ln p_s$ in spectral representation.

After expansion into Legendre functions (Eq. 5 in Segers et al., 2002a), the spectral fields are integrated numerically over the grid cell boundaries (for horizontal fluxes) or grid cell area (for average surface pressure and vertical flux).

Similar to the old procedure, a correction flux, $\mathbf{F}_l$, is obtained, separately and independent from the other layers, and is added to the horizontal fluxes in Eq. (7).

$$\boldsymbol{\delta}_h \cdot \mathbf{F}_l \; = \; - \left[m_l(t_1) - m_l(t_0) \right] / \Delta t \; - \; \boldsymbol{\delta}_h \cdot \mathbf{\Phi}_h(l) \; - \; \delta_l \Phi_w(l) \tag{7}$$

with δ_l as the vertical difference operator (see also Eq. 15 and 16 in Segers et al., 2002a). Note that now $\delta_l \Phi_w$ is explicitly included, representing the net vertical mass flux for every vertical layer, l.

1771

A small mass imbalance is still present between the mass tendency and the calculated vertical and horizontal mass fluxes. This mass imbalance cannot be avoided, since the meteorological fields represent a discrete time condition, whereas a CTM usually employs a specific time interval. In addition, the numerical integration contains

5 a limited accuracy.

3. Model evaluation

We have performed model experiments with two different versions of the TM3 model to evaluate the mass flux processing methods. First we calculated the mean age of air in the stratosphere with a tracer-pulse experiment. Next, we simulated a realistic ozone

10 distribution by integrations of the TM3 ozone tracer version. By calculating the mean age of air the large-scale circulation is examined. The ozone tracer experiment allows us to test the model performance on shorter time scales in regions with large tracer gradients and strong dynamical mixing. The model results have been compared with in situ observations.

15 3.1. Mean age of air experiment

The age spectrum, formally developed by Hall and Plumb (1994), is the probability distribution function of transit times of parcels from a source region to the sample region. This concept has shown to be a useful diagnostic for evaluating transport processes in global models (Hall et al., 1999). However, caution must be taken if a model evaluation

20 relies on the mean age of air only, since artifacts in different aspects of the circulation, which are not present in the mean age, may compensate (Schoeberl et al., 2002).

With a global transport model (CTM or GCM) the age spectrum is directly obtained from a passive tracer simulation where the mixing ratio in a small tropospheric volume is set equal to a delta-function in time. The source volume is located between 10° S

25 and 10° N in the lowest 8 models layers, up to about 800 hPa, where the initial mixing

ratio was set to one during the first model time step and zero hereafter. The response is then simply the age spectrum (Hall and Waugh, 1997). To allow the model to reach a stationary solution, the total simulation time was continued for 20 years, using the ECMWF meteorology of 1996 repeatedly.

5   Note that the mean age of air represents only the first moments of the age spectrum, and thus gives no information of higher moments or variability on shorter time scales (Hall et al., 1999). To evaluate the old and new mass flux processing methods, we therefore compared the modeled mean age of air with long-term mean observations only. Such data were derived from a 7-year average in situ CO_2 data record, sampled
10 on board the ER-2 aircraft (Andrews et al., 2001).

3.1.1. Comparison with observations

Figure 1 shows the zonally-averaged mean age of air at 20 km from both model simulations (with the old and new mass fluxes) and the observed mean age of air at 20 km altitude. The mean age derived with the old winds is significantly too small in the extra-
15 tropics, an earlier recognized problem that exists in many CTMs (Hall et al., 1999). The new method results in a mean age that is much closer to observations in the extra-tropics and illustrates a serious impact of the processing method. In the tropical region the air becomes somewhat older. Nevertheless, the calculated mean age of air remains too young in the extra-tropics.

20 ### 3.2. Ozone tracer experiment

This model version of TM3 contains an ozone tracer with prescribed ozone production and first- and second-order loss rates from a stratospheric 2-D model (Pitari et al., 1993). The tracer is constrained by an ozone climatology (Fortuin and Kelder, 1998) down to 50 hPa, scaled with 1996 Global Ozone Monitoring Experiment (GOME) total
25 ozone column data. More details of this version is given by Bregman et al. (2001). The studied year is 1996 and we will focus on the northern midlatitude UTLS (upper

troposphere and lower stratosphere).

Instantaneous 3-D model ozone fields have been compared with two sets of observations. One set contains ozone profiles from three ozone sounding stations (Hohenpeissenberg, Wallops Island, and Churchill), taken from the World Ozone Ultraviolet
5 Radiation Data Centre (WOUDC) at the Meteorological Service of Canada. The second data set includes ozone data from the two most frequently flown MOZAIC flight tracks in the northern midlatitudes, namely Frankfurt – New York (FRA-NEW) and Vienna – Tokyo (VIE-TOK) (Marenco et al., 1998). To compare the model results with the MOZAIC observations, seasonally averaged flight tracks were created and the model
10 ozone fields were interpolated to the aircraft location and pressure. The processing and comparison procedures are described in detail by Teyssèdre et al. [manuscript submitted to the Journal of Geophysical Research] and applied in Bregman et al. (2001).

3.2.1.   Comparison with observations

Figures 2,3 and 4 show results from comparisons with seasonally averaged ozone pro-
15 files from Wallops Island, Hohenpeissenberg, and Churchill. The new method yields significantly better agreement for the whole potential temperature (θ) range shown and at all three stations, especially at Churchill. The best agreement is found between θ levels of 330–370 K. Outside this layer considerable deviations remain, which probably illustrates the limitations of using a parameterized ozone chemistry scheme in the
20 model. Both at higher and lower θ levels photochemistry may play a more important role. In addition, uncertainties in the convection parameterization and the limited model grid resolution may become more critical in the upper troposphere.

Figures 5 and 6 show the results of a comparison between seasonally averaged model ozone mixing ratios ± one sigma ($\pm 1\sigma$) and MOZAIC observations for the 'mean'
25 flight FRA-NEW and VIE-TOK. The dashed lines represent the results when the old processing method is applied and are the same as the solid red lines in Plates 2 and 3 in Bregman et al. (2001). In Bregman et al. (2001) several CTMs and GCMs participated in a model intercomparison with the same model setup for the ozone integra-

tions as in this study. The flight track VIE-TOK is chosen because all models showed significant disagreement with observed mean mixing ratios and variability (the latter especially in summer) (Bregman et al., 2001).

A remarkable result is the good overall agreement for both mixing ratios and variability when the new processing method is used (solid lines). The large overestimate in all seasons, except for summer, has now disappeared. Even in summer the observed variability is well represented by our model.

3.3. Analysis of the vertical mass fluxes

To explain the differences between the model results using both processing methods we have analyzed the vertical mass fluxes. Figure 7 shows the zonal and yearly mean vertical mass flux and standard deviation at 200 and 100 hPa between 80 S and 80 N. The old winds contain stronger upward transport in the tropical region and stronger downward transport in the subtropical jet streams. This explains the older air in the tropical region using the new winds.

Older tropical air could also have been caused by enhanced lateral mixing with older extra-tropical air. However, given the steeper latitudinal gradient, enhanced meridional mixing does not seem to be present in the new winds. The meridional gradient, calculated with the new winds, remains nevertheless less steep than observed, indicating that the exchange between the tropics and extra-tropics may still be too strong. This has been found in other CTMs (Hall et al., 1999).

Note further that by using the meteorology of one particular year (1996), the calculated mean air age in the (sub)tropics may be underestimated, since the quasi-biennial oscillation (QBO) was in its easterly phase (Baldwin et al., 2001). On the other hand, the inter-annual variability of the age of air in the tropics is basically unknown, given the very limited observations (Waugh and Hall, 2002).

The winds derived by the old method most likely caused too much 'ventilation' or vertical mixing, an earlier reported shortcoming in CTMs (Schoeberl et al., 2002). Figure 7 indicates that vertical mixing is less pronounced using the new processing method and

thus leads to an older mean age of air.

Note that in the (sub)tropics the variability of the vertical mass flux at 200 hPa is slightly larger in the new winds, while it is significantly larger at middle and at high latitudes in the old winds. Especially for the ozone distribution in the tropopause region
the vertical mass flux variability is an important quantity as will be shown below.

The main causes for the differences in vertical mass flux variability between both methods are (i) interpolation of spectral data to a Cartesian grid and (ii) a mass correction by applying a distribution function based on the total vertically integrated mass. In the new method the surface pressure tendency is taken into account in the mass
balance equation for every vertical model layer. The old processing method therefore may introduce enhanced spurious variations in the vertical mass fluxes.

The weight of the interpolation errors increase when the grid cells become smaller, explaining the large increase of vertical mass flux variability closer to the poles with the old winds. By better representation of the winds the new method improves the
'real' mass flux variability. This is the most likely reason for the larger vertical mass flux variability in the tropical region using the new winds. The more realistic representation of mass flux variability is illustrated below.

Figure 8 shows the vertical mass flux variability (2σ) at 200 and 100 hPa for the winter period along all longitudes at 50 N. As shown for the zonal mean in Figure 7, the
old fluxes show larger variations than the new fluxes. A notable result in Figure 8 is the much clearer manifestation of orography using the new method. The two maxima that are present in the new fluxes indicate orographic effects (the Rocky Mountains and Tibetan high mountains). In reality orography induce enhanced vertical motion. The new method resolves this enhancement more accurate since the mass flux corrections
are performed per vertical layer independent from the other layers. In the old method the corrections are equally distributed in the vertical, leading to smearing out of the variability.

The important role of the vertical mass flux variability for modeled ozone is further illustrated by comparing winter with summer. In contrast to the winter situation, in

Mass conservation in global models

B. Bregman et al.

summer (see Fig. 9) the differences in mass flux variability between both methods are small, and so are the differences between modeled ozone distributions (see Figs. 2a–b). Hence, it seems that the difference in mass flux variability between both processing methods correlates with the differences in modeled ozone. The vertical mass flux variability is more pronounced in winter than in summer due to stronger and, most likely, more variable horizontal winds, associated with a larger latitudinal temperature gradient in winter.

Although observations for the MOZAIC flights were made close to the bottom edge of the large vertical ozone gradient near the tropopause. Fluctuations of the vertical mass flux will therefore lead to a net downward transport of ozone. This is the main reason for the large overestimation of ozone in the lowermost stratosphere when the old mass fluxes are used. Note that the annually average global downward ozone flux across the 150 hPa level is reduced from about 1700 Tg yr^{-1} (Bregman et al., 2001) to 850 Tg yr^{-1}. The latter flux is much better in agreement with estimates from observations reported in other studies (Murphy and Fahey, 1994).

Although in principle the new method applies to all models, the difference between the old and new method increases when the vertical levels are of a hybrid σ-pressure character. This partly explains why the differences between the old and new method in Figs. 7 and 8 are larger at 200 hPa than at 100 hPa. Above 100 hPa the vertical coordinates are fixed pressure levels, while they become increasingly sigma-like with increasing pressure.

4. Conclusions

A new mass flux processing method has been developed for chemistry-transport models. The method provides improved tracer-mass conserving wind fields, which solves the 'mass-inconsistency' problem, reported in earlier model studies. It takes into account spectral fields and the vertical flux changes in the mass balance equation for every vertical layer independently.

© EGU 2002

Two different versions of the TM3 model, a 3-D CTM with ECMWF meteorological fields to drive the transport, were used to evaluate the mass flux processing methods. One version contained an artificial tracer in a tracer-pulse experiment to calculate the mean age of air. The other version contained ozone as a tracer with a prescribed production and loss rates, constrained with an observed ozone climatology.

The calculated mean age of air and ozone distributions were compared with observations. The mean age of air is much better represented using the new mass fluxes, most likely caused by reduced vertical mixing. Nevertheless, the calculated mean age of air remains somewhat too young in the extra-tropical lower stratosphere. A potential cause is the limited representation of the large-scale stratospheric circulation when using a model top at 10 hPa. To investigate this, additional experiments with the new ECMWF re-analysis (ERA40) are currently underway.

The ozone distribution in the lower stratosphere shows better agreement with balloon observations, with the best agreement at θ levels between approximately 330–370 K. Outside this height range deviations remained, probably due to the limitation of the use of prescribed ozone chemistry. A striking improvement and excellent agreement with MOZAIC observations was found for ozone in the northern midlatitude tropopause region in all seasons over all longitudes, both in mean mixing ratios and variability.

By analyzing the vertical mass fluxes, most of the differences in modeled ozone and mean age of air between the old and the new processing methods could be explained. We have illustrated that the old mass flux processing method smooths out much of the real mass flux variability, while on the other hand it may create spurious variability. We have demonstrated that the model representation of the observations considerably improves when the spurious mass flux variability is decreased.

The problems reported here are probably not restricted to models that use assimilated meteorological data to drive the transport. In many Eulerian climate models spectral wind fields are transformed into mass fluxes to perform the advection of tracers. For these models, as well as for off-line models, it is recommended that the vertically integrated mass divergence is made consistent with the surface pressure changes. All

relevant terms, including $\nabla \ln p_s$, should be calculated using their spherical harmonic representation. Finally, a `FORTRAN90` code of the new processing algorithm is available at http://www.knmi.nl/~segers.

References

Andrews, A., Boering, K., Daube, B., Wofsy, S., Loewenstein, M., Jost, H., Podolske, J., Webster, C., Herman, R., Scott, D., Flesh, G., Moyer, E., Elkins, J., Dutton, G., Hurst, D., Moore, F., Ray, E., Romanshkin, P., and Strahan, S.: Mean ages of stratospheric air derived from in situ observations of CO_2, CH_4, and n_2o, J. Geophys. Res., 106, 32 295–32 314, 2001. 1773, 1782

Baldwin, M., Gray, L., Dunkerton, T., Hamilton, K., Haynes, P., Randel, W., Holton, J., Alexander, M., Hirota, I., Horinouchi, T., Jones, D., Kinnersley, J., Marquardt, C., and Takahasi, M.: The quasi-bienial oscillation, Rev. Geophys., 39, 179–229, 2001. 1775

Bregman, A., Krol, M., Teyssèdre, H., Norton, W., Chipperfield, M., Pitari, G., Sundet, J., and Lelieveld, J.: Chemistry-transport model comparison with ozone observations in the midlatitude lowermost stratosphere, J. Geophys. Res., 106, 17 479–17 496, 2001. 1767, 1769, 1773, 1774, 1775, 1777

Dentener, F., Feichter, J., and Jeuken, A.: Simulation of the transport of Rn^{222} using on-line and off-line global models at different horizontal resolutions: A detailed comparison with measurements, Tellus, 51, 573–602, 1999. 1768

Fortuin, J. and Kelder, H.: An ozone climatology based on ozonesonde and satellite measurements, J. Geophys. Res., 103, 31 709–31 734, 1998. 1773

Hall, T. and Plumb, R.: Age as a diagnostic of stratospheric transport, J. Geophys. Res., 99, 1059–1070, 1994. 1772

© EGU 2002

Hall, T. and Waugh, D.: Timescales for the stratospheric circulation derived from tracers, J. Geophys. Res., 102, 8991–9001, 1997. 1773

Hall, T., Waugh, D., Boering, K., and Plumb, R.: Evaluation of transport in stratospheric models, J. Geophys. Res., 104, 18 815–18 839, 1999. 1772, 1773, 1775

5 Heimann, M.: The Global Atmospheric Tracer Model TM2, Tech. Rep. 10, DRKZ-Hamburg, 1995. 1767, 1768, 1769

Heimann, M. and Keeling, C.: A three-dimensional model of atmospheric CO_2 transport based on observed winds: 2: Model description and simulated tracer experiments, Geophys. Mon., 55, 237–275, 1989. 1767, 1768, 1769

10 Houweling, S., Dentener, F., and Lelieveld, J.: The impact of non-methane hydrocarbon compounds on tropospheric photochemistry, J. Geophys. Res., 103, 10 673–10 696, 1998. 1768

Jöckel, P., von Kuhlmann, R., Lawrence, M., Steil, B., Brenninkmeijer, C., Crutzen, P., Rasch, P., and Eaton, B.: On a fundamental problem in impelmenting flux-form advection schemes for tracer transport in 3-dimensional general circulation and chemistry transport models, Q.
15 J. R. Meteorol. Soc., 127, 1035–1052, 2001. 1767

Marenco, A., Thouret, V., Nedelc, P., Smit, H., Helten, M., Kley, D., Karcher, F., Simon, P., Law, K., Pyle, J., Poschmann, G., von Wrede, R., Hume, C., and Cook, T.: Measurement of ozone and water vapor by airbus in-service aircraft: The MOZAIC airborne program, an overview, J. Geophys. Res., 103, 25 631–25 642, 1998. 1774

20 Murphy, D. and Fahey, D.: An estimate of the flux of stratospheric reactive nitrogen and ozone into the troposphere, J. Geophys. Res., 99, 5325–5332, 1994. 1777

Peters, W., Krol, M. C., Dentener, F. J., and Lelieveld, J.: Identification of an El Niño-Southern Oscillation signal in a multiyear global simulation of tropospheric ozone, J. Geophys. Res., 106, 10 389–10 402, 2001. 1768

25 Pitari, G., Rizi, V., Ricciardulli, L., and Visconti, G.: High-speed civil transport impact: Role of sulfate, nitric acid trihydrate, and ice aerosols studied with a two-dimensional model including aerosol physics, J. Geophys. Res., 98, 23 141–23 164, 1993. 1773

Prather, M.: Numerical advection by conservation of second-order moments, J. Geophys. Res., 91, 6671–6681, 1986. 1769

30 Schoeberl, M., Douglass, A., Zhu, Z., and Pawson, S.: A comparison of the lower stratospheric age-spectra, derived from a General Circulation Model and two data assimilation systems, J. Geophys. Res., submitted, 2002. 1772, 1775

Segers, A., van Velthoven, P., Bregman, B., and Krol, M.: On the computation of mass fluxes for

Eulerian transport models from spectral meteorological fields, in: Proceedings of the 2002 International Conference on Computational Science, Lecture Notes in Computer Science (LNCS), Springer Verlag, 2002a. 1769, 1770, 1771

Segers, A., van Velthoven, P., Bregman, B., and Krol, M.: Computation of mass fluxes for Eulerian transport models from spectral meteorological fields, J. Comput. Phys., submitted, 2002b. 1769, 1770

Stockwell, D. and Chipperfield, M.: A tropospheric chemical-transport model: Development and validation of the model transport schemes, Q. J. R. Meteorol. Soc., 125, 1747–1783, 1999. 1767

Van den Broek, M., Bregman, A., and Lelieveld, J.: Model study of stratospheric chlorine and ozone loss during the 1996/1997 winter, J. Geophys. Res., 105, 28 961–28 977, 2000. 1768

Waugh, D. and Hall, T.: Age of stratospheric air: theory, observations, and models, Reviews of Geophysics, in press, 2002. 1775

Mass conservation in global models

B. Bregman et al.

© EGU 2002

Mass conservation in global models

B. Bregman et al.
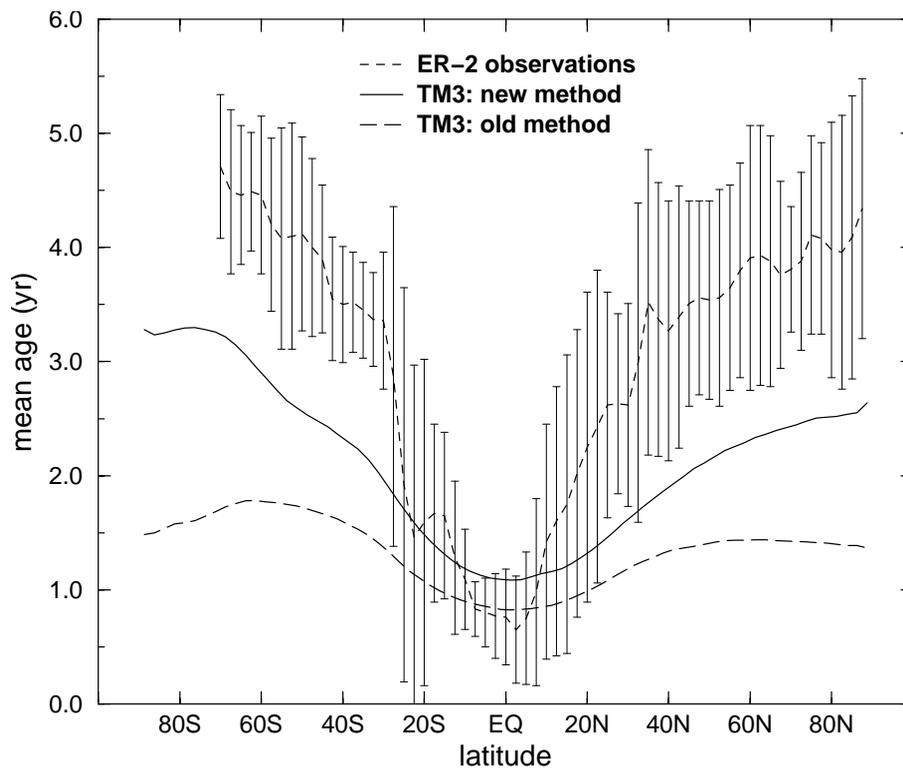
Fig. 1. Observed mean age of air at 20 km altitude, compiled from all ER-2 CO_2 data from 1992 and 1998 (dashed line), including the error bars ($\pm 2\sigma$) (Andrews et al., 2001). The model results are shown by the dashed (old method) and solid (new method) lines.
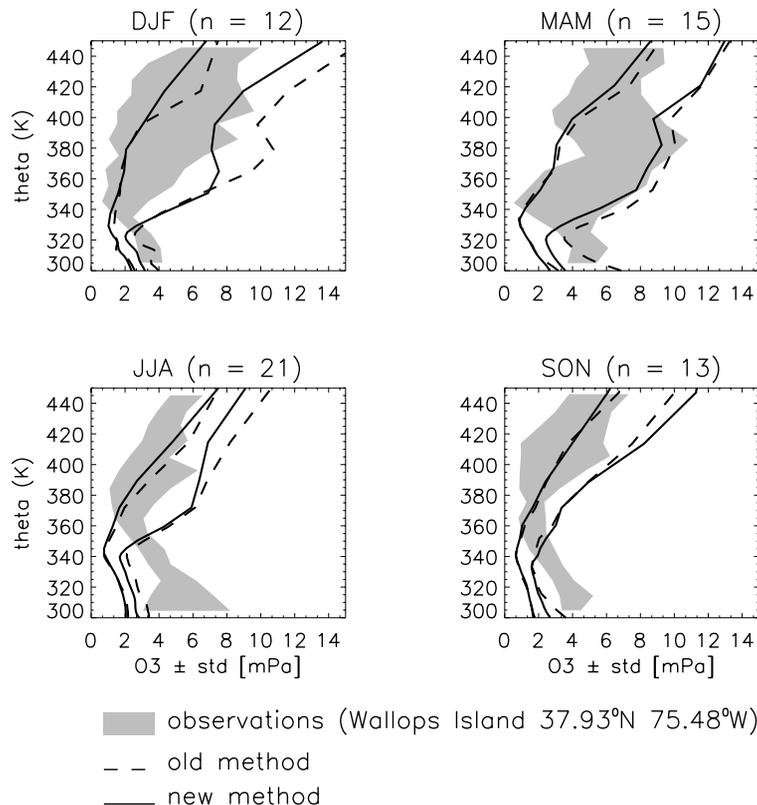
Fig. 2. Seasonal mean ozone partial pressure (mPa) $\pm 1\sigma$ from ozone sonde observations (filled grey) at Wallops Island. The dashed and solid lines represent the model results using the old and new mass flux processing method respectively. The vertical axis is represented by the potential temperature [K].

Mass conservation in global models

B. Bregman et al.

Fig. 3. Similar as Fig. 2, but for Hohenpeissenberg.

Title Page

Abstract | Introduction

Conclusions | References

Tables | Figures

◄◄ | ►►

◄ | ►

Back | Close

Full Screen / Esc

Print Version

Interactive Discussion

© EGU 2002
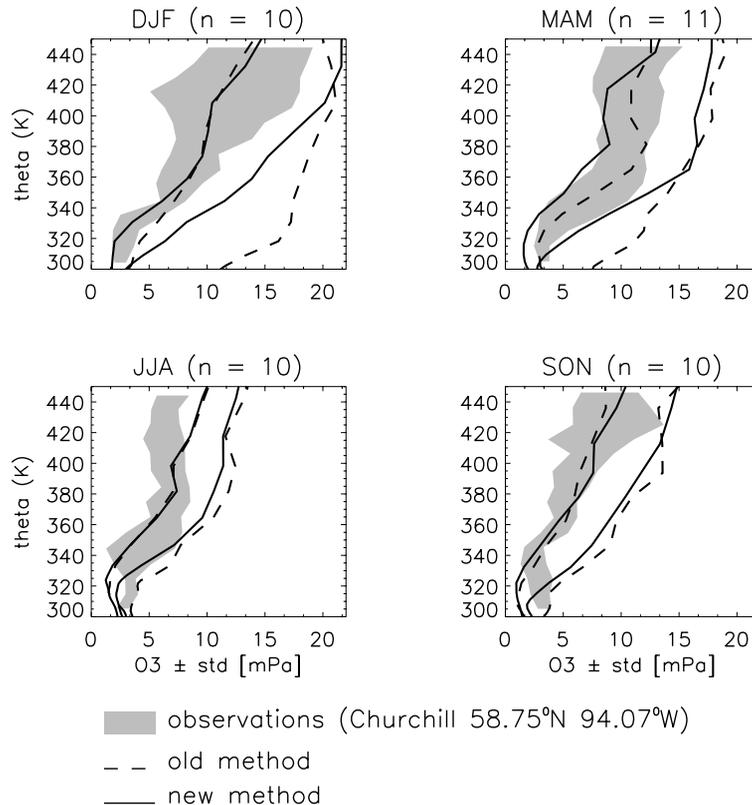
Fig. 4. Similar as Fig. 2, but for Churchill.

Title Page

| Abstract | Introduction |

| Conclusions | References |

| Tables | Figures |

◄◄   ►►

◄   ►

Back   Close

Full Screen / Esc

Print Version

Interactive Discussion
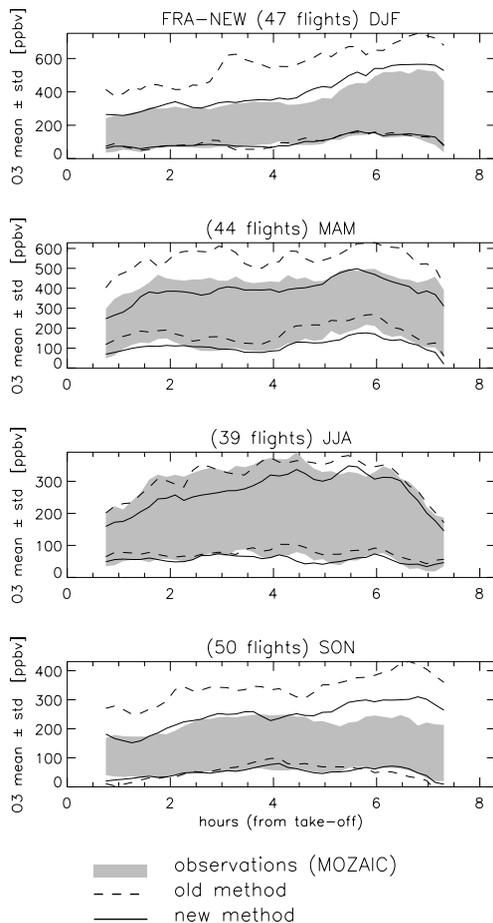
Fig. 5. Seasonal mean ozone mixing ratios (ppbv) (±1σ), as observed during the MOZAIC project for the flight Frankfurt – New York (filled grey), and calculated by the model using the old (dashed) and the new (solid) mass flux processing method.

Fig. 6. Similar as Fig. 5, but for the flight Vienna - Tokyo.

Title Page

Abstract | Introduction

Conclusions | References

Tables | Figures

◄◄ | ►►

◄ | ►

Back | Close

Full Screen / Esc

Print Version

Interactive Discussion

© EGU 2002
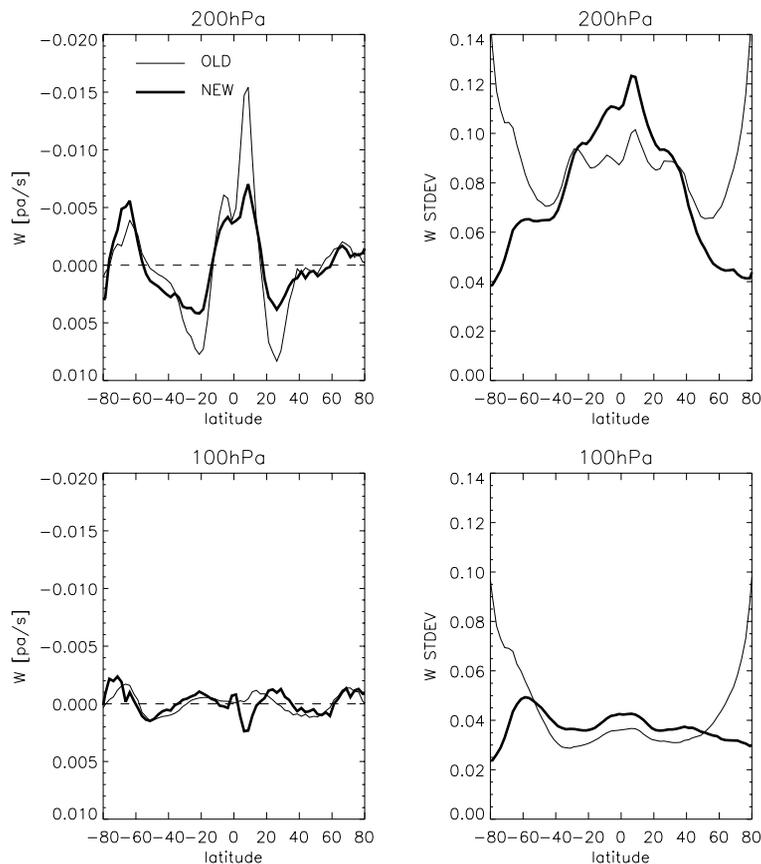
Fig. 7. Yearly and zonal mean vertical mass flux (Pa s^{-1}) and standard deviation (±2σ) calculated by the model at 100 and 200 hPa, using the old (thin solid lines) and the new (thick solid lines) mass flux processing method.

Title Page

Abstract | Introduction

Conclusions | References

Tables | Figures

◄◄ | ►►

◄ | ►

Back | Close

Full Screen / Esc

Print Version

Interactive Discussion
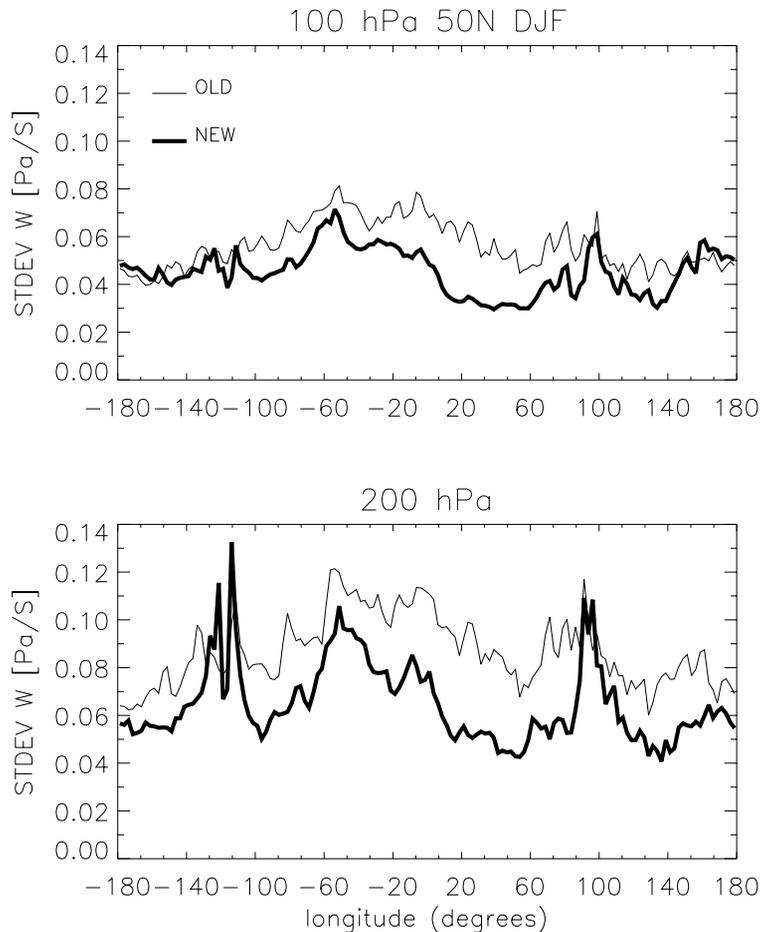
Fig. 8. Standard deviation (2σ) of the calculated vertical mass flux (Pa s^{-1}) at 50°N and two different pressure levels (100 and 200 hPa) in December, January, and February (DJF), using the old (thin solid lines) and the new (thick solid lines) mass flux processing method.

Mass conservation in global models

B. Bregman et al.

Title Page	
Abstract	Introduction
Conclusions	References
Tables	Figures
◄◄	►►
◄	►
Back	Close
Full Screen / Esc	

Print Version

Interactive Discussion

© EGU 2002
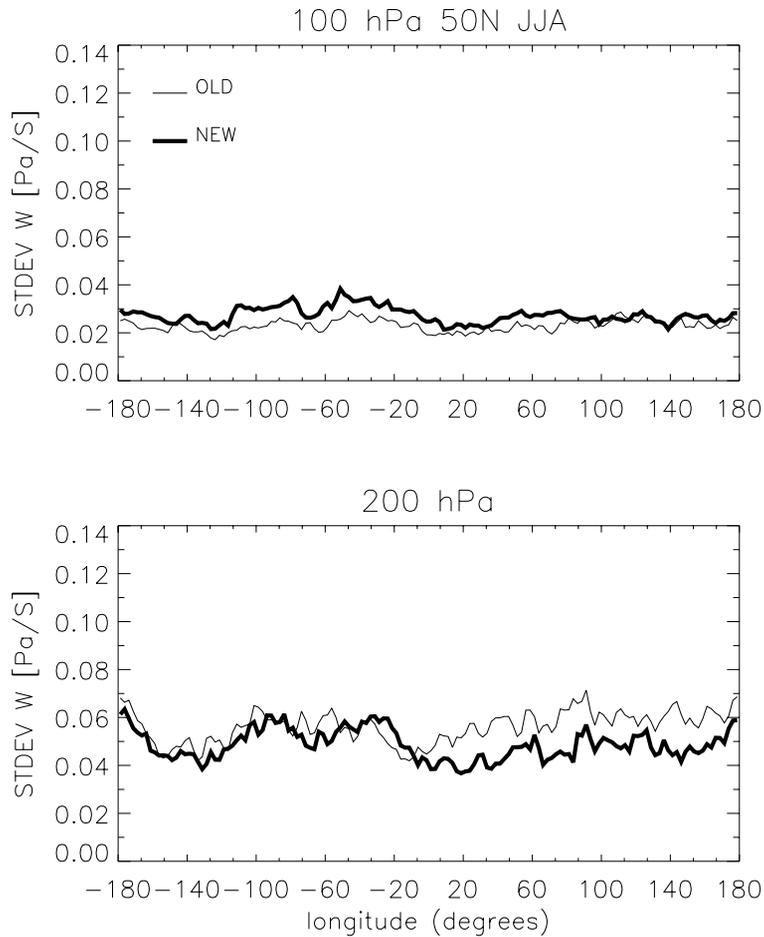
Fig. 9. Similar as Fig. 8, but for June, July, and August (JJA).